

Caenorhabditis elegans TRPA-1 functions in mechanosensation

Katie S Kindt^{1,2,6}, Veena Viswanath^{3,5,6}, Lindsey Macpherson⁴, Kathleen Quast², Hongzhen Hu³, Ardem Patapoutian^{3,4} & William R Schafer^{1,2}

Members of the transient receptor potential (TRP) ion channel family mediate diverse sensory transduction processes in both vertebrates and invertebrates. In particular, members of the TRPA subfamily have distinct thermosensory roles in *Drosophila*, and mammalian TRPA1 is postulated to have a function in noxious cold sensation and mechanosensation. Here we show that mutations in *trpa-1*, the *C. elegans* ortholog of mouse *Trpa1*, confer specific defects in mechanosensory behaviors related to nose-touch responses and foraging. *trpa-1* is expressed and functions in sensory neurons required for these mechanosensory behaviors, and contributes to neural responses of these cells to touch, particularly after repeated mechanical stimulation. Furthermore, mechanical pressure can activate *C. elegans* TRPA-1 heterologously expressed in mammalian cells. Collectively, these data demonstrate that *trpa-1* encodes an ion channel that can be activated in response to mechanical pressure and is required for mechanosensory neuron function, suggesting a possible role in mechanosensory transduction or modulation.

Sensory neurons convert environmental stimuli into an electrical signal. Sensory receptor proteins of diverse modalities from various species have been isolated, including taste and odorant receptors. Relatively little is known about thermo- and mechanoreceptors. *C. elegans* respond to temperature gradients and show several genetically distinct mechanosensory responses. However, the molecular mechanisms underlying transduction of these behaviors remain relatively unknown.

One of the first sensory modalities to be explored in detail in *C. elegans* was response to body touch (reviewed in ref. 1). Both light body touch (stroking the worm's body with an eyelash) and harsh body touch (touching the body with a platinum wire) evoke an escape behavior in which the direction of the locomotion wave rapidly changes to allow the worm to crawl away from the mechanical stimulus. These responses have been characterized in detail by laser ablation studies, genetic analyses, *in vivo* imaging and electrophysiology. Three neurons (ALML, ALMR and AVM) are required for reverse locomotion in response to anterior touch, and two neurons (PLML and PLMR) are required for forward acceleration away from posterior touch². Seventeen genes required for response to gentle body touch have been isolated, and are designated 'mec' (mechanosensory abnormal) genes³. The products of at least three of these genes, the stomatin MEC-2, the degenerin-epithelial Na⁺ channel (DEG/EnaC) protein MEC-4, and the accessory protein MEC-6, comprise core components of a mechanotransduction complex. Expression together of these molecules in heterologous cells reconstitutes an ion channel⁴ that is permeable to sodium as well as calcium⁵. Mutations in any of

these genes specifically abolish neural responses to gentle touch in intact worms⁶ and mechanoreceptor potentials in dissected worm preparations⁷. The products of the other *mec* genes are thought to function in coupling the opening of this mechanoreceptor complex to mechanical forces applied to the body cuticle¹.

C. elegans also shows distinct mechanosensory responses to mechanical stimulation of the nose ('nose-touch')⁸. An eyelash placed in the path of a forward-moving worm evokes a reversal upon collision, a behavior dependent on the ASH nociceptive neurons as well as at least two additional neuron classes, OLQ and FLP. OSM-9, a member of the vanilloid subfamily of transient receptor potential (TRPV) family in *C. elegans*, is required for this nose-touch avoidance behavior, as well as for escape responses to several noxious stimuli⁹. *osm-9* mutants are also defective in ASH neural responses to all mechanical, chemical and osmotic stimuli tested, though whether OSM-9 is a direct sensor of these stimuli is not known.

Touch modulates other aspects of *C. elegans* behavior, including the behavior known as foraging¹⁰. On a plate with food, *C. elegans* make high frequency, local exploratory movements of the head known as foraging. Touching the nose or the anterior body of foraging worms with an eyelash results in backward movement and interruption of foraging^{10,11}. The OLQ and IL1 neurons are required for normal foraging behavior; ablation of these neurons results in exaggerated head bends and slower foraging rate¹⁰. Additionally, touch to the ventral or dorsal side of the nose results in an aversive head withdrawal reflex^{10,12}. The OLQ and IL1 sensory neurons are also required for

¹MRC Laboratory of Molecular Biology, Hills Road, Cambridge CB2 2QH, UK. ²Division of Biology, University of California, San Diego, 9500 Gilman Drive, La Jolla, California 92093, USA. ³Genomics Institute of the Novartis Research Foundation, 10675 John Hopkins Road, San Diego, California 92121, USA. ⁴Department of Cell Biology, ICND202, The Scripps Research Institute, 10550 North Torrey Pines Road, La Jolla, California 92037, USA. ⁵Present address: Allergan, Inc., 2525 Dupont Drive, Irvine, California 92623, USA. ⁶These authors contributed equally to this work. Correspondence should be addressed to A.P. (apatapou@gnf.org) or W.R.S. (wschafer@mrc-lmb.cam.ac.uk).

this behavior and are thought to mediate the primary sensory response by signaling through the RMD motor neurons¹⁰. However, the identity of the mechanotransduction channel mediating these responses is not known.

There is increasing evidence that transient receptor potential (TRP) ion channels have important roles in transduction of temperature and pressure^{13,14}. TRPA ion channels, the most recently identified TRP subfamily, has members in various phyla, including vertebrates and invertebrates. Initial studies showed that noxious cold temperature activates TRPA1, the single mammalian member of this subfamily¹⁵. Indeed, TRPA1 seems to be required for mediation of cold hyperalgesia after peripheral inflammation due to complete Freund adjuvant (CFA) or nerve injury in rats¹⁶. Notably, vertebrate TRPA1 has also been identified as a candidate for the mechanosensitive transduction channel in vertebrate hair cells¹⁷. Two recent studies of *Trpa1*^{-/-} mice found no defects in auditory responses^{18,19}. One of these studies¹⁹ but not the other¹⁸ found *Trpa1*^{-/-} mice to have a lowered sensitivity to noxious cold and mechanical stimuli, implying a role in somatosensory thermo- and mechanotransduction¹⁹. The TRPA subfamily includes four *D. melanogaster* and two *C. elegans* members²⁰. Two members of the Drosophila TRPA family, TrpA1 and pyrexia, have been shown to be required for different modes of temperature sensation^{20–22}. painless, a more distant Drosophila TRPA family member, has been shown by genetic analysis to mediate high-temperature mechanical responses²³. The role of the *C. elegans* TRPA subfamily has not been characterized.

In this study we describe the identification and characterization of *C. elegans* TRPA-1. We show that TRPA-1 is required for normal mechanosensory responses of *C. elegans* to nose-touch and for normal foraging behavior, but is not essential for other mechanosensory, thermosensory or chemosensory behaviors tested here. When expressed in Chinese hamster ovary cell line (CHO) cells, TRPA-1 is activated by mechanical stimuli, supporting a role of TRPA-1 in mechanosensation in worms.

RESULTS

C. elegans TRPA-1 is expressed in many sensory neurons

Our homology searches identified two TRPA1 family members in *C. elegans* (Supplementary Fig. 1 online). One, *C. elegans* TRPA-1 (41% similarity, 23% identity to mouse TRPA1), is an ortholog of mouse TRPA1 and *D. melanogaster* TRPA1; the other, TRPA-2, is a distant family member with no predicted ankyrin domains. (Alignment is shown in Supplementary Fig. 2 online.) Given the suggested roles of TRPA family members in thermosensation and mechanosensation in other species, we focused on *C. elegans trpa-1*. Similarly to other members of this family, *trpa-1* encodes a putative ion channel, TRPA-1, with six predicted transmembrane domains and 17 predicted N-terminal ankyrin repeats¹⁴.

To establish where *trpa-1* is expressed, we constructed reporter transgenes consisting of translational fusions of the *trpa-1* gene to green fluorescent protein (GFP). We generated three such fusion gene constructs, all containing the entire 2.5 kb intergenic sequences between *trpa-1* and upstream gene F38H4.10. In addition, constructs contained either the first two exons (the 'short fusion'), the first six exons (the 'partial protein fusion') or all 11 exons (the 'full-length protein fusion') of *trpa-1* fused in-frame to GFP (Fig. 1a). For all three constructs, multiple transgenic lines were used to confirm expression; one line was examined in detail.

We observed expression of TRPA-1::GFP fusion proteins in several cell types. In lines carrying the short fusion construct (for example, *ljEx107*), TRPA-1::GFP fusion protein was localized to many tissues, including pharyngeal muscle and body wall muscle, the excretory

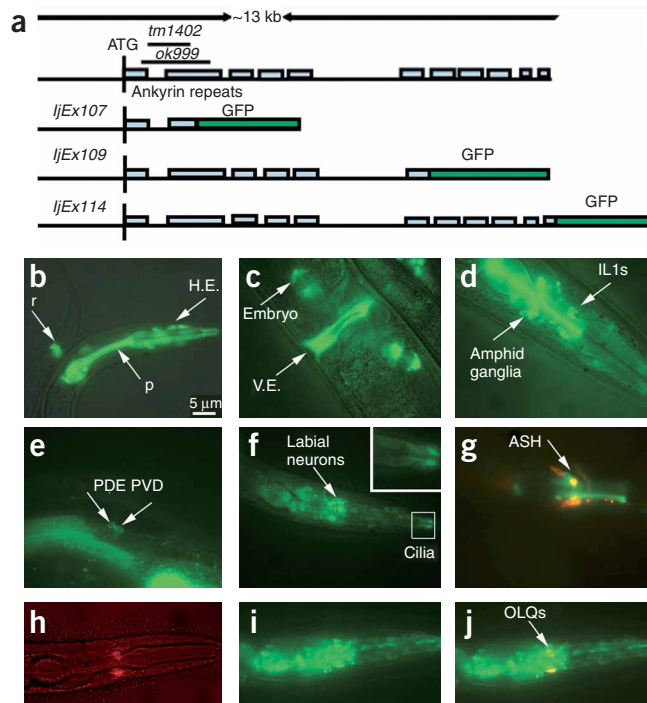


Figure 1 TRPA-1::GFP fusion protein is expressed in neuron and non-neuronal cell types. (a) The design of the three TRPA-1::GFP fusion constructs, with ~2.5 kb of promoter sequence and the first 3, 6 or all 11 exons (denoted as blue boxes) of *trpa-1* fused to GFP. (b) Expression of the *ljEx107* fusion gene. Expression is observed in the rectal gland (r), head epithelium (H.E.) and pharynx (p). (c) Expression of *ljEx114* in the non-neuronal tissue of the vulva epithelium (V.E.) and also in an embryo. (d,e) Expression of *ljEx114* in the IL1 neurons in the amphid ganglia in the head, and in the PVD and PDE neurons in the postdeirid ganglia. (f) Expression of *ljEx114* in the labial neurons OLQ and IL1 with an inset of expression in the cilia enlarged to 225% of its former size. (g) DiI staining showing colocalization of *ljEx114* in the ASH neuron. (h–j) Expression of *pocr-4::RFP* in the OLQ neurons (h), *ljEx114* (i) and a merged image (j) of i and h, showing expression of *ljEx114* in the OLQ neurons. In all pictures, anterior is to the right and ventral to the bottom (except ventral projects out in c).

system, the rectal gland cell, vulval epithelium, epithelial cells in the head, and the spermatheca (Fig. 1b,c and data not shown). We also observed sporadic expression in some head neurons with this construct. Transgenic lines generated with the partial and full-length protein fusion constructs (for example, *ljEx109* and *ljEx114* respectively) expressed TRPA-1::GFP in the same cells as *ljEx107* (Fig. 1b,c), but with some additional cells, including the majority of amphid sensory neurons (for example, ASH, AWA, AWB, ASI and ASK) and the phasmid neurons PHA and PHB (Fig. 1d and data not shown). The full-length TRPA-1::GFP fusion was also expressed in the PVD and PDE in the postdeirid sensilla (Fig. 1e) and the sensory neurons OLQ and IL1 (Fig. 1d,f). Other neurons in the head and ventral nerve cord also expressed TRPA-1::GFP (data not shown). Notably, we observed the fusion protein at the cilia of sensory neurons (Fig. 1f), as well as at the cell body.

The ASH, OLQ, IL1 and FLP neurons are known to contribute to reversal and head withdrawal responses to nose-touch. We therefore sought to verify expression of TRPA-1 in these cells through colocalization experiments. We confirmed that TRPA-1::GFP was expressed in ASH by labeling worms with the lipophilic dye DiI, which labels ASH

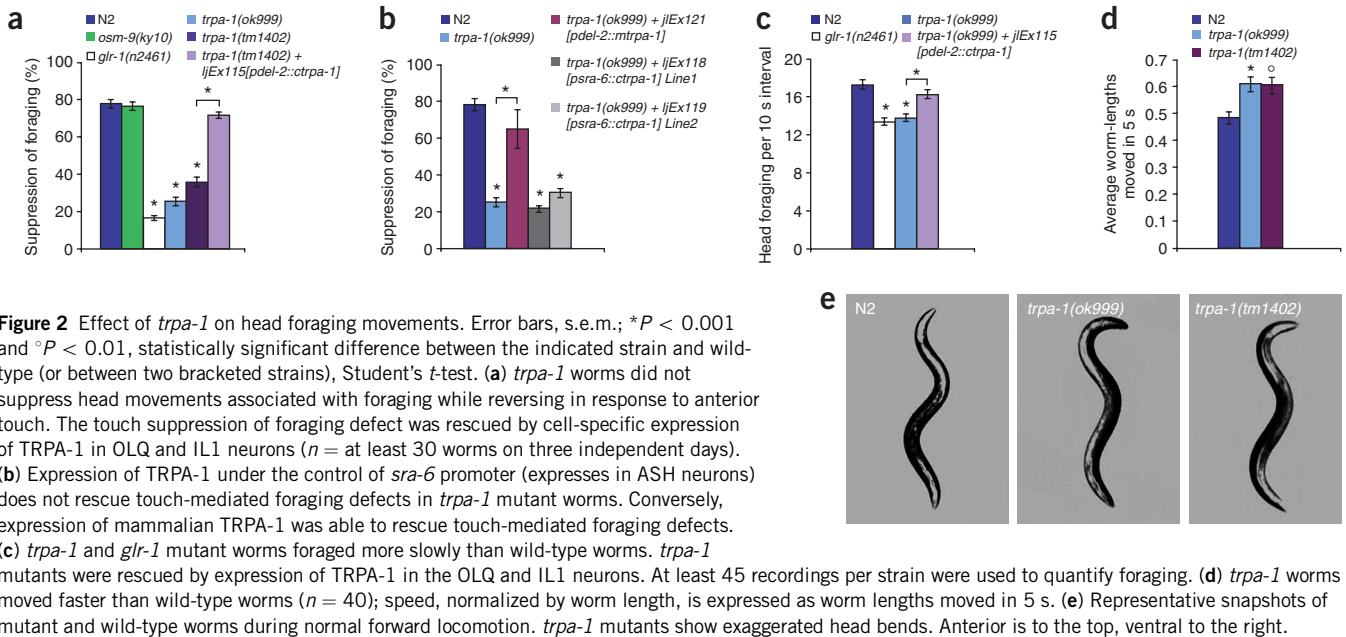


Figure 2 Effect of *trpa-1* on head foraging movements. Error bars, s.e.m.; * $P < 0.001$ and $^{\circ}P < 0.01$, statistically significant difference between the indicated strain and wild-type (or between two bracketed strains), Student's *t*-test. (a) *trpa-1* worms did not suppress head movements associated with foraging while reversing in response to anterior touch. The touch suppression of foraging defect was rescued by cell-specific expression of TRPA-1 in OLQ and IL1 neurons ($n =$ at least 30 worms on three independent days). (b) Expression of TRPA-1 under the control of *sra-6* promoter (expresses in ASH neurons) does not rescue touch-mediated foraging defects in *trpa-1* mutant worms. Conversely, expression of mammalian TRPA-1 was able to rescue touch-mediated foraging defects. (c) *trpa-1* and *glr-1* mutant worms foraged more slowly than wild-type worms. *trpa-1* mutants were rescued by expression of TRPA-1 in the OLQ and IL1 neurons. At least 45 recordings per strain were used to quantify foraging. (d) *trpa-1* worms moved faster than wild-type worms ($n = 40$); speed, normalized by worm length, is expressed as worm lengths moved in 5 s. (e) Representative snapshots of mutant and wild-type worms during normal forward locomotion. *trpa-1* mutants show exaggerated head bends. Anterior is to the top, ventral to the right.

through its exposed sensory cilia. (Fig. 1g). We did not detect expression of TRPA-1::GFP in the FLP nose-touch neurons (identified by the pattern of nuclei visualized by differential interference contrast (DIC) optics²⁴). To assess expression in the OLQ neurons among the many labial neurons, we generated a red fluorescent protein (RFP) reporter construct using the promoter of the *del-2* gene to generate transgenic animal expressing *pdel-2*::RFP (Supplementary Fig. 3 online). The *del-2* promoter is reported to be specifically expressed in the IL1, OLQ, and possibly the ASH neurons⁸. In our hands *pdel-2*::RFP expression was seen in the IL1 and OLQ labial neurons, though we did not detect expression in any amphid neurons (See note in Supplementary Results and Methods online). Similarly we also generated a *pocr-4*::RFP construct, which was specifically expressed in OLQ (Fig. 1h–j)²⁵. Both RFP reporters labeled TRPA-1::GFP-expressing labial neurons, confirming that TRPA-1 is expressed in the known nose-touch neurons ASH and OLQ, as well as in the putatively mechanosensory IL1 neurons.

trpa-1 mutants show foraging defects

To determine the role of *trpa-1* *in vivo* we next examined the behavior of mutants defective in this ion channel. We obtained two mutations expected to cause a loss of TRPA-1 function, *ok999* and *tm1402*. The *ok999* allele deletes about 1,400 bp encoding the N-terminal region of the predicted protein, whereas *tm1402* harbors a 581-bp deletion and a 16-bp insertion at the 5' end of the *trpa-1* coding sequences. We did not detect a cDNA product in reverse transcriptase–polymerase chain reaction (RT-PCR) experiments from mutants carrying either of these alleles when we used primers that amplify wild-type full-length *trpa-1* (data not shown). We also performed RT-PCR from a downstream ATG at 1,987 bp in the gene and likewise did not obtain any detectable messages (data not shown). The two alleles of *trpa-1* mutants were viable and healthy and had normal brood size (though there was a slight developmental delay in the *trpa-1(ok999)* allele). We broadly surveyed the behavior of the *trpa-1* mutants, and observed normal or nearly normal phenotypes with respect to thertotaxis, gentle and harsh body touch; a subtle abnormality in egg-laying; and abnormal pharyngeal pumping (Supplementary Fig. 4, Supplementary Results

and Supplementary Methods online). These results led us to believe that discernment of the *trpa-1*'s function in these cells might require more sophisticated behavioral assays.

The expression of the full-length *trpa-1* reporter transgene in the OLQ and IL1 neurons prompted us to examine in *trpa-1* mutants two behaviors known to be strongly dependent on these neurons, foraging and the head withdrawal reflex. In the presence of food, *C. elegans* make rapid nose oscillations termed 'foraging' as they explore their environment. These oscillations cease upon touch to the top of the nose or anterior body^{10,11}. When worms are touched on the ventral or dorsal side of the nose during forward movement they respond with an aversive head movement away from the stimulus, termed the head withdrawal reflex¹⁰. Both foraging and the head withdrawal reflex are impaired by ablation of the OLQ and IL1 labial neurons and their synaptic target the RMD motor neurons¹⁰. Likewise, *glr-1* mutants (which are defective in a glutamate receptor that functions in RMD) have abnormal head withdrawal reflex and foraging behaviors¹⁰ (also see Fig. 2). Neither the *mec-4* DEG/ENaC ion channel required for body touch response nor the *osm-9* TRPV ion channel mediating nose-touch response in ASH seem to be required for head withdrawal or foraging (Fig. 2a and data not shown). Thus, the identity of the primary mechanotransduction channel mediating these behaviors in OLQ and IL1 is not known.

When we assayed the effect of mutations in *trpa-1* on foraging behaviors, we observed that both *trpa-1* mutant strains (*ok999* and *tm1402*) did not suppress foraging when touched on top of the head or anterior body (28% suppression, compared with 85% in wild-type; Fig. 2a). This phenotype was rescued by expression of wild-type *trpa-1* in OLQ and IL1 under the control of the *del-2* promoter (Fig. 2a) but not in ASH under the control of the *sra-6* promoter (Fig. 2b), consistent with previous work suggesting that ASH is not involved in this behavior¹⁰. Notably, the mouse *Trpa1* gene expressed under the control of the *del-2* promoter (*ljEx121 [pdel-2::mtrpa-1]*) also partially rescued the nose-touch suppression of foraging phenotype of *trpa-1* mutant worms (Fig. 2b).

OLQ and IL1 have also been shown to affect the frequency and amplitude of foraging movements. We observed that *trpa-1(ok999)*, like

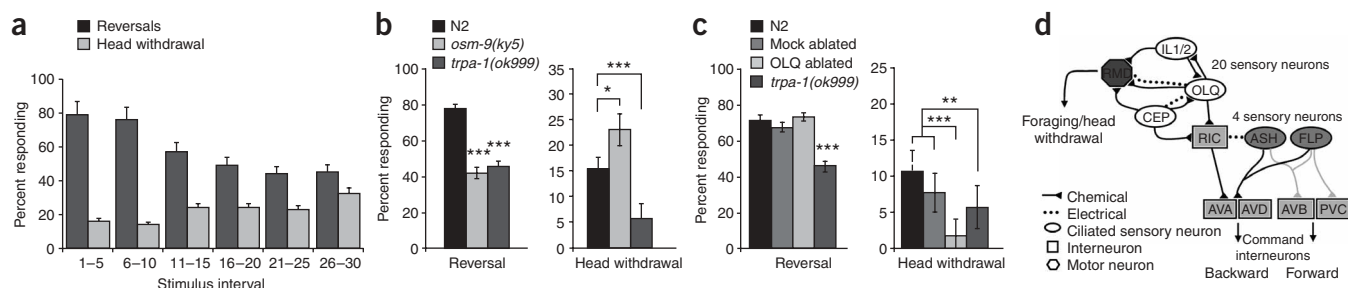


Figure 3 *trpa-1* mutants are defective in the head withdrawal reflex. Error bars, s.e.m.; *** $P < 0.001$, ** $P < 0.001$ and * $P < 0.01$, Student's *t*-test. (a) Both reversal response and head withdrawal can be seen in wild-type nose touch stimulations. Head withdrawal becomes more apparent with repeated stimulation ($n = 20$). Even within the first ten nose touch stimulations, *trpa-1* mutants are defective in head withdrawal, while *osm-9* mutants show an elevated frequency of head withdrawals compared with wild-type (b). (b) Response of wild-type worms to ten consecutive nose-touch stimulations. (c) Ablation of OLQ neurons has no effect on the reversal response to nose-touch but similar to *trpa-1* mutants, the frequency of head withdrawals in OLQ-ablated worms are significantly reduced compared with wild-type or mock-ablated worms. $n = 10$ worms for N2, mock and ablated; each worm was scored in three sets of ten stimulations. $n = 30$ for *trpa-1* mutants. (d) A schematic of the nose-touch circuit. FLP and ASH mechanoreceptors exert main effects directly on the command interneurons, to inhibit forward movement (light chemical synapses) and activate backward movement (dark chemical synapses). OLQ and IL1 labial neurons form part of an interconnected network of 20 ciliated putative mechanosensory neurons. This network forms synapses on the RMD motor neuron to directly modulate head movement and foraging, and also synapses onto the interneuron RIC to indirectly activate the backward command interneurons to modulate reversal behavior.

glr-1 mutants, foraged at a significantly slower rate than wild-type (Fig. 2c), a phenotype that was rescued by expression of wild-type *trpa-1* under the *del-2* promoter (Fig. 2c). This slow foraging rate was not a result of overall slow locomotor activity, as *trpa-1* mutants moved at a slightly faster rate compared with wild-type (Fig. 2d). *trpa-1* mutants also showed exaggerated head bends during foraging (Fig. 2e), a phenotype observed in worms with ablated OLQ and IL1 neurons¹⁰.

We also observed in *trpa-1* mutants defects in the head withdrawal reflex, another behavior mediated by the OLQ and IL1 neurons. Head withdrawal was previously reported to occur after gentle touch to the side of the nose¹⁰. We were also able to reliably score head withdrawal in response to nose-touch by placing an eyelash perpendicular to the path of the worm during forward movement⁸. In response to a nose-on collision with an eyelash, we observed two distinct responses: a reversal, in which the worm crawled backward away from the stimulus, or a head withdrawal. Initially, most wild-type worms (~80%) responded to nose-touch with a reversal (Supplementary Video 1 online, Fig. 3a,b), and fewer (~15%) respond with a head withdrawal (Supplementary Video 2 online, Fig. 3a,b). Head withdrawal behavior became more prominent with repeated nose-touches (Fig. 3a). Using this assay, we

found that *trpa-1* mutants showed a significant reduction in the head withdrawal response (Fig. 3b). A similar result was observed when we ablated the OLQ neurons (Fig. 3c,d), consistent with previous results implicating OLQ in the head withdrawal reflex¹⁰.

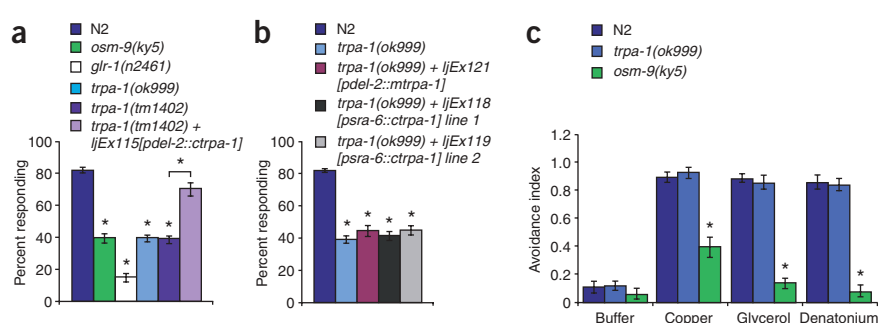
In summary, *trpa-1* mutants showed multiple phenotypes characteristic of OLQ- and IL1-ablated worms, indicating a possible role for TRPA-1 in these putative mechanosensory neurons. The OLQ and IL1 neurons in the two *trpa-1* mutant strains had normal morphologies (data not shown), suggesting that *trpa-1* affects the function rather than the structure or development of these cells.

trpa-1 mutants are also defective in response to nose-touch

In addition to being defective in head withdrawal in response to nose-on collision with an eyelash, we found that *trpa-1* mutants were also defective in reversal behavior in response to nose-touch (Figs. 3b and 4a). Ablation experiments have implicated the putative mechanoreceptor neurons OLQ and FLP, along with the ASH nociceptors, in this behavior⁸.

To determine in what neurons TRPA-1 was affecting nose touch, we assayed whether reversal behavior defects in response to nose-touch

Figure 4 *trpa-1* mutants have defects in reversal response to nose-touch, but are normal for ASH-mediated osmosensory and chemosensory avoidance behaviors. Each data point represents at least 30 worms, assayed on three independent days. Error bars, s.e.m.; * $P < 0.001$ significantly different from wild-type, except in the *pdel-2::trpa-1* rescue experiment, * $P < 0.001$ different from *trpa-1* mutant; Student's *t*-test for nose-touch experiments, χ^2 test for the drop test. (a) Reversal response of wild-type and *trpa-1(ok999)* and *tm1402* worms after nose-touch. The *trpa-1* mutants show a compromised response to nose-touch, which is rescued by expression of TRPA-1 in the labial sensory neurons IL1 and OLQ neurons. Nose-touch-insensitive *osm-9* mutants (defective in the ASH TRPV channel) and *glr-1* mutants served as controls. (b) Expression of TRPA-1 specifically in ASH neurons (in the two independent lines, *lJEx118* and *lJEx119*) under the control of *sra-6* promoter is not able to rescue the nose-touch phenotype of the *trpa-1*. Similarly, expression of mammalian TRPA1 in the IL1 and OLQ neurons does not rescue the nose-touch defects of the *trpa-1* mutants. (c) In a drop-test assay *trpa-1* mutants avoid heavy metals (1 mM copper chloride), high osmotic strength (1 M glycerol) and bitter compounds (10 mM denatonium) to the same degree as wild-type worms. *osm-9(ky10)*, which abolishes all ASH sensory responses, served as control.



were rescued by expression of TRPA-1 under the control of promoters specific to ASH or other nose-touch neurons. To assess functional rescue in ASH, we used the *sra-6* promoter, which expresses strongly in ASH and weakly in ASI²⁶. In two independent rescue lines, *ljEx118* and *ljEx119*, we observed no complementation of the *trpa-1* nose-touch phenotype (Fig. 4b). We also assayed rescue using a fragment of the *del-2* promoter, which directed expression as previously reported⁸ in the OLQ and IL1 neurons, though not in ASH (see note in Methods). We observed that *trpa-1* mutant worms expressing [*pdel-2:trpa-1(+)*] were rescued significantly for reversal behavior in response to nose-touch (Fig. 4a). Similar results were seen for the *trpa-1(ok999)* allele (data not shown). Next, we tested whether mammalian TRPA1 could also rescue *trpa-1* nose-touch defects. In this case, expression of mouse *Trpa1* in the OLQ and IL1 neurons did not restore nose-touch avoidance in the *trpa-1* mutants (Fig. 4b). This is in contrast to the ability of mouse *Trpa1* to rescue the touch-mediated foraging behaviors in the *trpa-1* mutant (Fig. 2b). This implied that the mechanistic role of TRPA-1 in foraging responses to nose-touch might be different from its role in reversal responses.

The TRPV channel subunits encoded by *osm-9* and *ocr-2* have been shown to be required in the ASH nociceptors for reversals in response to nose-touch, as well as other ASH-detected repellents. In contrast, although *trpa-1* mutants were defective for the nose-touch-evoked reversal behavior, unlike the *osm-9* and *ocr-2* mutants, *trpa-1* worms did not show defects in other ASH-mediated avoidance behaviors. For example, *trpa-1* worms showed normal avoidance of high osmolarity, denatonium and Cu²⁺ (Fig. 4c). The selectivity of the sensory defects in *trpa-1* worms implied that TRPA-1 was not required for general aspects of ASH function and development, and therefore most likely either had a modality specific function in ASH or, alternatively, functioned primarily in other nose-touch sensory neuron.

Together, these results suggested that TRPA-1 functioned in the OLQ and/or IL1 neurons, but not in ASH, to facilitate foraging rate and both head withdrawal and reversal response to nose touch. Notably, eliminating the OLQ neurons alone with a laser microbeam strongly affects head withdrawal and foraging, but does not significantly disrupt the reversal response to nose-touch⁸ (see also Fig. 3c). Thus, whereas the head withdrawal and foraging phenotypes of *trpa-1* mutants were consistent with a function primarily in the OLQ and possibly IL1 neurons, its effect on the reversal response to nose-touch may imply an additional function for the TRPA-1 channel in other neurons required for this behavior (see Fig. 3d).

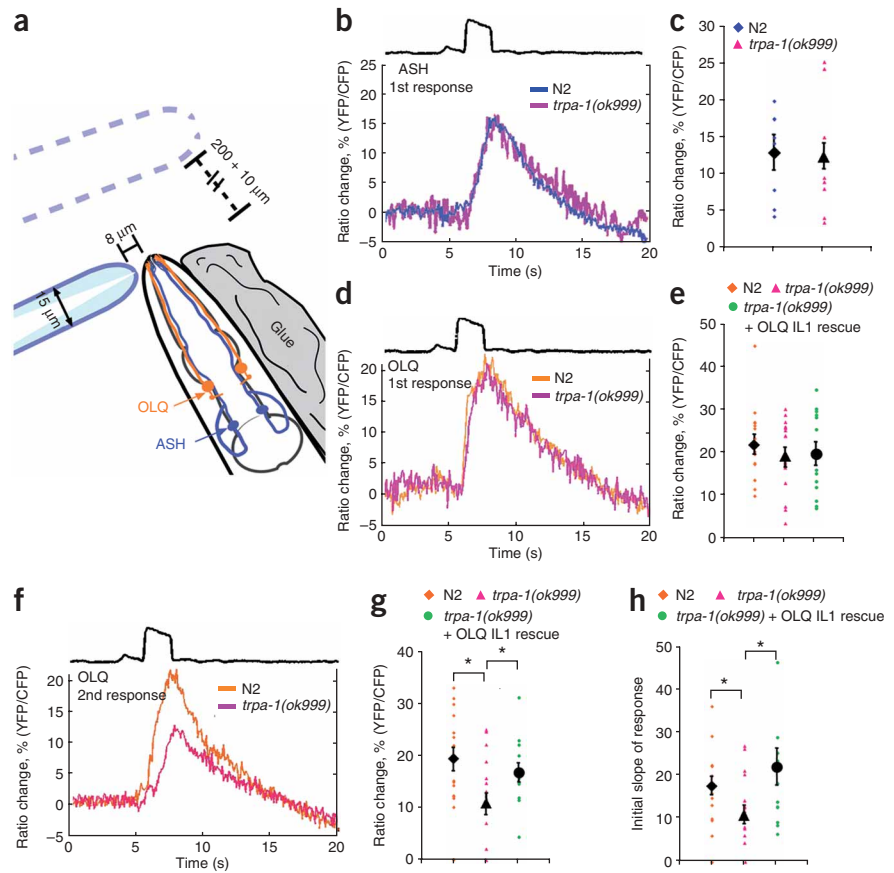


Figure 5 Effects of *trpa-1* on neural responses to nose-touch in OLQ and ASH. Error bars, s.e.m.; nonparametric Mann-Whitney rank sum test, * $P < 0.05$. (a) Schematic of imaging setup for nose-touch stimulation. Worms expressing cameleon in either the ASH (blue) or OLQ (orange) neurons were immobilized with glue and immersed in a bath solution containing 2 mM serotonin. To stimulate, a glass probe ($\sim 10 \mu\text{m}$ tip) was displaced $8 \mu\text{m}$ into the side of the nose, held for 2 s and then released. Dashed probe, previous stimulation tactics. (b,c) Representative (b) and quantitative summary (c) of ASH recordings from wild-type and *trpa-1* mutant worms ($n = 8$). Traces indicate YFP/CFP ratio, which correlates with intracellular calcium. The black line indicates duration of nose touch. (d,e) Representative (d) and quantitative (e) nose-touch responses of wild-type and *trpa-1* mutant in the OLQ neuron in response to initial nose-touch stimulations. No significant difference was observed. (f) Representative nose-touch in OLQ in response to a subsequent stimulation (5-min delay from initial stimulation) in wild-type and *trpa-1* mutants. (g,h) Quantification of subsequent OLQ nose-touch responses in wild-type, *trpa-1* mutants, and *trpa-1* mutants expressing *C. elegans trpa-1* in the OLQ and IL1 neurons ($n = 15, 18$ and 13 respectively). *trpa-1* mutants show a significantly reduced response compared with wild-type (g) and the initial slope of the nose-touch response is higher in wild-type worms (h). Expressing *trpa-1* in the OLQ and IL1 neurons rescues these defects (g,h).

trpa-1 affects neural responses of OLQ neurons to nose-touch

To determine how TRPA-1 might affect mechanosensory responses in the nose, we used the genetically encoded calcium sensor cameleon to monitor *in vivo* responses of the ASH and OLQ neurons to touch stimuli (Fig. 5a). We showed previously that ASH shows cell-autonomous calcium transients in response to nose-touch that are dependent on the TRPV channel *osm-9* (ref. 27). Using the *ljEx95[psra-6::YC2.12]* cameleon line, which expresses cameleon in ASH, we tested the effect of *trpa-1* mutations on touch-induced calcium transients in these cells²⁷. We observed no significant difference between either *trpa-1* mutant alleles and wild-type (Fig. 5b,c), indicating that TRPA-1 may not be critically important for nose-touch transduction in ASH.

We also tested neural responses to nose-touch in OLQ. We generated a cameleon line, *ljEx130[pocr-4::YCD3]*, that expressed cameleon

specifically in OLQ under the control of the *ocr-4* promoter. Using this line, we observed reproducible responses to nose-touch stimuli in wild-type worms. When *trpa-1* mutants were tested in this assay, there was no significant difference in calcium transients compared with wild-type (21.6% for wild-type versus 19.1% for *trpa-1*; Fig. 5d,e) in response to an initial nose-touch stimulation. However, in response to a second nose-touch stimulation recorded 5 min after the first, *trpa-1* mutants showed a dramatically reduced response compared with the wild-type second response (19.6% for wild-type versus 10.6% for *trpa-1*; Fig. 5f,g). In addition, the initial slope of the ratio change, which indicates the rate of calcium influx, was also significantly reduced compared with wild-type for the second nose-touch response (17.9 versus 11.0, Fig. 5h). Both of these defects could be rescued by expressing *trpa-1* cell-specifically in the OLQ and IL1 neurons (Fig. 5g,h). In contrast, these difference were not seen in *trpa-1* ASH secondary nose touch responses.

Measurements of baseline fluorescence intensity and YFP/CFP ratio did not show significant differences between *trpa-1* mutant worms and wild-type (Supplementary Fig. 5 online); however, we cannot rule out the possibility that effects of *trpa-1* on calcium dynamics or homeostasis might contribute to the observed differences in touch induced calcium transients. Nonetheless, these data indicate that *trpa-1* contributes to the physiological responses of these neurons to touch, potentially as either a mechanotransducer or a modulator of sensory adaptation. We were unable to conduct similar experiments for the IL1

neurons, as *cameleon* lines using known IL1 promoters (for example, *del-2*) were insufficiently bright to be useful for imaging.

Worm TRPA-1 is activated by mechanical stimuli in CHO cells

To test whether *C. elegans* TRPA-1 could be activated by mechanical stimulation, we established a stable tetracycline (tet)-inducible TRPA-1 CHO cell line and assayed electrophysiological responses to pressure from the recording pipette. Application of pressure stimuli to cells using the recording electrode has been previously used to study mechanosensitive ion channels^{28–30}. It is hypothesized that pressures applied to whole cells mimic the pressure a cell experiences during mechanical stimulation^{30,31}. Negative pressure applied to the cell from the recording pipette results in cell shrinkage. For example, a cell's observed two dimensional area decreases to 89.5% of its original size after applying a -50 mm Hg suction (Supplementary Fig. 6 online). In whole-cell recordings, we observed robust currents in response to suction stimuli (negative pressure) in TRPA-1-expressing stable CHO cells induced with tet ($n = 22$), but not in uninduced control cells ($n = 15$) (Fig. 6a,b). The threshold of TRPA-1 activation was estimated to be -44 ± 5 mm Hg suction ($n = 25$, \pm s.e.m.). The average current density evoked by -100 mm Hg at $+100$ mV was 7.47 ± 2.19 pA pF^{-1} ($n = 22$, \pm s.e.m.) in tet-induced TRPA-1 expressing CHO cells, and 0.98 ± 0.39 pA pF^{-1} ($n = 15$, \pm s.e.m.) in uninduced TRPA-1 cells (Fig. 6c). Complementing the results obtained from the stably transfected tet-inducible TRPA-1 CHO cells, -100 mm Hg pressure applied

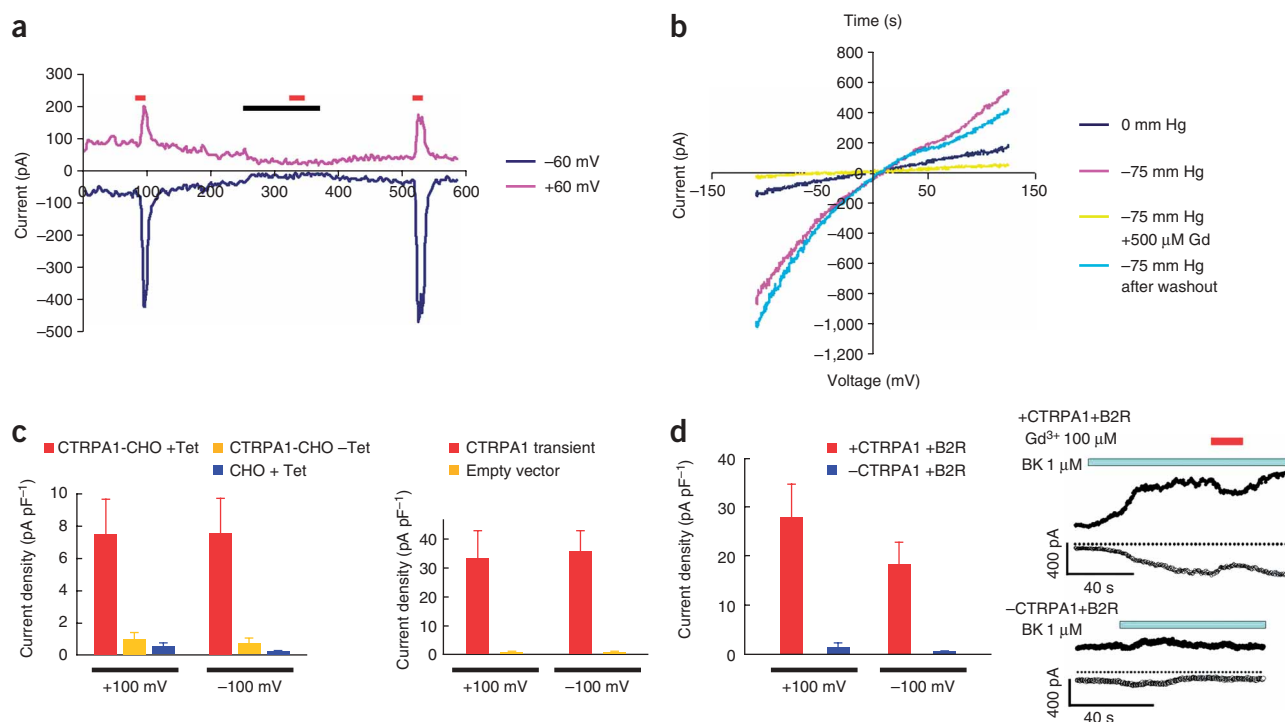


Figure 6 Mechanical stimuli activate TRPA-1-expressing CHO cells. (a) TRPA-1-expressing CHO cells respond to suction in whole-cell configuration. Application of -75 mm Hg suction (red bar) activates a representative TRPA-1-expressing CHO cell; $500 \mu\text{M}$ Gd^{3+} (black bar) blocks the suction-induced currents. Currents are shown at holding potentials of $+60$ and -60 mV. (b) Instantaneous current voltage relationships of the same cell shown above. Voltages were ramped from -120 to $+120$ mV. Responses are shown before and during application of -75 mm Hg suction with and without $500 \mu\text{M}$ Gd^{3+} in the bath. (c) Average current density evoked by an average suction of -100 mm Hg. Left, current densities in tet-induced and uninduced CHO cells stably expressing TRPA-1 as well as naive CHO cells treated with Tet at ± 100 mV. $n = 22$, 15 and 15 for TRPA-1 + Tet, TRPA-1 - Tet and CHO + Tet, respectively. Right, current densities in CHO cells transiently transfected with TRPA-1 ($n = 10$) or empty vector ($n = 11$). (d) Left, average current density evoked by $1 \mu\text{M}$ bradykinin (BK) in transiently transfected HEK cells transfected with both TRPA-1 and bradykinin receptor (B2R) (+TRPA-1 + B2R, $n = 16$) or with B2R alone (-CTRPA1 + B2R, $n = 14$). Right, representative traces of a +TRPA-1 + B2R cell responding to $1 \mu\text{M}$ bradykinin, partially and reversibly inhibited by $100 \mu\text{M}$ Gd^{3+} (top trace) and a -TRPA-1 + B2R cell's response to $1 \mu\text{M}$ bradykinin (bottom trace). Error bars, \pm s.e.m.

to CHO cells transiently transfected with TRPA-1 elicited similar currents (Fig. 6c). TRPA-1-expressing cells did not respond to positive pressure stimuli—that is, to blowing (up to +50 mm Hg). Positive pressures > 50 mm Hg disrupt the integrity of the seal and were not tested. We did not observe responses to hypotonic or hypertonic solutions in TRPA-1-expressing CHO cells. We also did not observe any responses in a stable cell line expressing mouse TRPM8 ($n = 7$) or in tet-treated naive CHO cells ($n = 15$) (data not shown and Fig. 6c). The currents evoked by mechanical stimuli in TRPA-1-expressing cells show dual rectification, similar to those observed for other members of the TRP superfamily³² (Fig. 6b). We observed a reversal potential of 0 mV. Responses to prolonged suction stimuli showed no desensitization (Supplementary Fig. 6). Cells expressing TRPA-1 did not respond to any of the sensory compounds that have previously been shown to activate mammalian TRPA1, such as cinnamaldehyde, mustard oil or allicin (data not shown)^{33,34}.

We also assayed TRPA-1 responses to pharmacological antagonists of mammalian TRP channels. Ruthenium red, a blocker of several thermosensory TRP channels, did not block TRPA-1. Previous studies have shown that ruthenium red acts by binding to a negatively charged aspartate in the putative pore of the TRP channels³⁴. Consistent with this, sequence analysis revealed that this aspartate is not conserved in the pore of TRPA-1. Gadolinium (Gd^{3+}) is considered a blocker of native mechanically gated ion channels in animal tissues and has been previously shown to block mouse TRPA1^{32,35–37}. Gd^{3+} at 500 μM completely blocked suction responses of TRPA-1 cells (3 of 3 cells), whereas 100 μM Gd^{3+} partially blocked TRPA-1 currents ($51 \pm 4\%$ of activated levels; 3 of 10 cells were completely blocked, 4 of 10 partially blocked and 3 of 10 not blocked) (Fig. 6a,b, and data not shown). Application of 500 μM Gd^{3+} caused a reduction of the basal currents owing to blockade of constitutive activity of TRPA-1 (Fig. 6a,b). This is similar to the effect of 100 μM Gd^{3+} on mouse TRPA1 expressed in HEK cells and the effect of 10 mM camphor on rat TRPA1 expressed in HEK cells^{36,38}. However, application of 500 μM Gd^{3+} had no effect on uninduced TRPA-1 CHO cells (Supplementary Fig. 6). These results imply that TRPA-1 is a nonselective cation channel similar to other members of this family and that it is activated by mechanical stimuli.

Finally, we explored whether TRPA-1 could be activated by mechanisms independent of mechanical stimuli. Some TRP ion channels are activated downstream of G protein-coupled receptors³⁹. Bradykinin is an inflammatory peptide that mediates pain and inflammation. Mouse TRPA1 is activated by bradykinin through the Bradykinin 2 receptor³⁴. In similar fashion, worm TRPA-1 is activated by bradykinin-receptor activation in CHO cells (Fig. 6d). This activity can be partially blocked ($45 \pm 9\%$) by 100 μM Gd^{3+} and is not observed in the absence of TRPA-1 (Fig. 6d).

DISCUSSION

We have shown here that *trpa-1*, the *C. elegans* TRPA1 ortholog, is activated in response to a mechanical stimulus *in vitro* and contributes to mechanosensory responses *in vivo*. Loss-of-function mutations in *trpa-1* cause abnormalities in distinct behaviors requiring the labial mechanosensory neurons: nose-touch-evoked escape behavior, both in reversal response and head withdrawal; control of foraging amplitude and frequency; and touch-mediated suppression of foraging behavior. These phenotypes are rescued by expression of the wild-type *trpa-1* gene under the control of a *del-2* promoter, which seems to be specific to the OLQ and IL1 neurons. In addition, *trpa-1* mutations significantly alter neural responses of OLQ (but not ASH) to nose-touch stimuli. However, unlike other *C. elegans* mechanosensory channels,

such as the TRPV channel OSM-9 (ref. 27) and the DEG/ENaC channel MEC-4 (ref. 6), which are absolutely required for touch responses in the ASH and ALM neurons respectively, TRPA-1 is less essential for sensory responses, at least in OLQ. In particular, TRPA-1 seems to be more important for responding to a repeated stimulus than for responding to a single stimulus.

What mechanistic role might TRPA-1 have in the process of mechanosensation in OLQ? As *C. elegans* TRPA-1 protein expressed heterologously in mammalian cells forms ion channels that are activated by a mechanical stimulus, one possibility is that TRPA-1 is a direct mechanosensor, but that its activity is at least partially redundant for nose-touch responses in the labial neurons. For example, in *Drosophila* hair mechanoreceptors, there seems to be a minor mechanoreceptor potential that is independent of the *nomp C* TRPN channel⁴⁰. Alternatively, as the OLQs receive synaptic input (Fig. 2d) from the CEP neurons that behavioral²⁴ and calcium imaging experiments indicate are mechanosensory (K.S.K. and W.R.S., unpublished observations), the *trpa-1*-independent response to nose-touch may in part involve indirect activation of OLQ by the CEPs. In either of these models, one would hypothesize that the TRPA-1 function makes a more significant contribution to OLQ responses after repeated stimulation.

Alternatively, it is possible that TRPA-1 does not mediate sensory transduction directly, but rather has a modulatory role in the OLQ mechanosensory neurons. In particular, it is possible that TRPA-1 regulates the kinetics of sensory adaptation. We have shown that worm TRPA-1, like many other TRP channels, can be activated downstream of G protein-coupled receptor (GPCR) activation as well as by mechanical stimuli. Thus, a role for TRPA-1 in mechanosensory adaptation might involve second-messenger control of TRPA-1 activity rather than, or in addition to, direct mechanical activation. In this regard we note with interest that OSM-9, the TRPV channel required for mechano- and chemosensory transduction in ASH, affects sensory adaptation rather than transduction in a variety of other neurons in which signaling is G protein-coupled receptor dependent⁹. Further studies should provide insight into how TRP channels might participate in the control of sensory adaptation.

The *trpa-1* behavioral defect in nose-touch behaviors might seem surprisingly strong given the partial defect in OLQ neural responses. However, it should be noted that the neural phenotype of *trpa-1* is much stronger after repeated stimulation, and as standard nose-touch assays involve testing the responses of a single worm to multiple stimulations, the behavioral defect may be correspondingly stronger. There is also precedent for partial losses of neural response having strong effects on behavior: for example, loss-of-function mutants for *odr-3*, a G-protein α -subunit thought to activate OSM-9 TRPV channels in ASH⁴¹, have strong behavioral defects in ASH-mediated avoidance behaviors, even though the mutations reduce repellent-evoked calcium transients by only about 50% (ref. 27). It is also reasonable to suppose that *trpa-1* function in the IL1 neurons may also contribute to the nose-touch avoidance phenotype, though we were unable to test this directly because of the lack of a suitable *cameleon* line.

It is instructive to compare the role of TRPA-1 in nose-touch behavior with the molecules involved in a different *C. elegans* mechanosensory behavior, gentle body touch. Two members of the amiloride-sensitive DEG/ENaC sodium channel family (MEC-4 and MEC-10) and a stomatin protein (MEC-2), as well as several other proteins required for gentle body touch avoidance, are hypothesized to form a mechanotransduction complex in the ALM, AVM and PLM neurons⁴². Although *in vivo* imaging and electrophysiology have demonstrated that the core components of this putative complex are specifically

required for gentle touch mechanotransduction by the body touch neurons^{6,7}, heterologously expressed DEG/ENaC channels have not been shown to be mechanosensitive⁴, which may indicate a requirement for additional factors such as intracellular or extracellular tethers. In contrast, we have found that TRPA-1 is activated in response to mechanical forces applied to a recording patch pipette. Although we have not shown here that TRPA-1 is directly gated by mechanical stimulation (and it is possible that the mechanical forces activate TRPA-1 indirectly through release of membrane-associated or cytosolic factors^{43,44}), this result indicates that TRPA-1 is functional without any specialized accessory molecules not already present in CHO cells. This may reflect a fundamental difference in the mechanisms of touch sensation in TRPA-expressing neurons and DEG/ENaC expressing neurons.

It is also instructive to compare the role of TRPA-1 with previously characterized TRPV ion channels, which are also required for mechanosensory and chemosensory avoidance behaviors. The *osm-9* and *ocr-2* genes, members of the TRPV family, are required for reversal responses to nose-touch, though not for foraging responses. In addition, *osm-9* and *ocr-2* mutants have defects in osmotic and chemical avoidance, and imaging experiments indicate that they are required for nose-touch and other sensory responses in ASH neurons^{25,27}. In contrast to what we have observed here for TRPA-1, activation of OSM-9 or OCR-2 by mechanical stimuli has not been demonstrated in heterologous systems, and in fact some of the functions of OSM-9 and OCR-2 are dependent on G protein-mediated signaling pathways²⁵. Thus, the mechanisms by which TRPV channels participate in mechanosensory transduction may also differ in important ways from those of TRPA channels.

In addition to the labial mechanosensory neurons, many other cells express *trpa-1*, including many neurons. However, no strong behavioral phenotypes could be attributed to expression in these cells. In particular, *trpa-1* mutations had no detectable effect on the sensory functions of ASH, despite clear expression of *trpa-1* reporters in these neurons. Perhaps TRPA-1 has a minor or modulatory role in sensory transduction in ASH, or alternatively functions in some other aspect of cellular physiology. In this regard, we note that the TRPV channel *osm-9* also has a broad expression pattern in *C. elegans*, including neuronal and non-neuronal cells⁹. In at least some of these cells (for example, the olfactory neuron AWA), OSM-9 channels are localized to the neuronal cell body rather than the sensory cilia, and function in sensory adaptation rather than sensory transduction^{9,25}. As TRPA-1, like other TRP channels in various phyla³⁷, can couple with GPCRs, it is possible that TRPA-1 may have functions in some neurons that are distinct from its mechanosensory activity.

The role of the TRPA family of ion channels in sensory biology is now well established in many systems, from nematodes to mammals (this study, and reviewed in ref. 13). But whereas these results implicate *trpa-1* in *C. elegans* in mechanosensation, TRPA family members in other animals were initially implicated as thermosensory channels. For example, mouse and fly TRPA1 proteins are activated by temperature, and loss-of-function mutants are defective in thermosensory behaviors^{15,16,19–21}. However, a potential role for mammalian TRPA1 in mechanosensation was recently suggested by the observation that mice lacking TRPA1 have a deficit in acute somatic mechanosensation¹⁹. Notably, expression of mouse TRPA1 in the OLQ and IL1 neurons rescued the touch-mediated foraging but not the nose-touch avoidance behaviors in the *trpa-1* mutants. Combined, TRPA1 orthologs from three species are shown to be critical in sensing cold, heat, and mechanical stimuli. Understanding the molecular mechanisms by which TRPA channels are regulated by such distinct sensory stimuli represents an important and fascinating challenge for future investigation.

METHODS

Molecular cloning of worm TRPA-1. We performed phylogenetic analysis of the TRPA family among the various genomes as previously described²². Using RT-PCR, a 3.6-kb *trpa-1* cDNA was amplified from adult *C. elegans* RNA using the primers 5'-ATGTCGAAGAAATCATTAGG-3' and 5'-TCAGTTATCTTTC TCCTCAAGT-3'. A feature of this cDNA not predicted in Wormbase is a coding exon of 82 bp that is 525 bp upstream of the predicted start ATG. PCR rapid amplification of cDNA ends (Clontech) was used to confirm the 5' end of *trpa-1*.

Generation of TRPA-1 GFP expression constructs and transgenic worms. We used the GFP expression vector pPD95.75 (A. Fire) to construct all TRPA-1::GFP fusions. To generate TRPA-1 GFP translational fusion constructs, 2.5 kb of promoter sequences plus the first two exons (for TRPA-1exon2::GFP), the first six exons (for TRPA-1exon6::GFP) or all the genomic sequences of TRPA-1 with GFP fused in frame just before the STOP codon (for TRPA-1full::GFP) was amplified by PCR and subcloned into the pPD95.75 vector. *ljEx107* was created by injecting TRPA-1exon2::GFP at 50 ng μl^{-1} into a *lin-15* mutant using 50 ng μl^{-1} *lin-15* rescue plasmid as a transformation marker. *ljEx109* was created by injecting both TRPA-1exon6::GFP at 50 ng μl^{-1} and *lin-15(+)* rescue plasmid at 50 ng μl^{-1} into a *lin-15* mutant. *ljEx114* was generated by injecting TRPA-1full::GFP into the N2 strain at 35 ng μl^{-1} . Each line was compared with one or to two additional independent transgenic lines with the same reporter to confirm the expression pattern.

Generation of RFP and cameleon constructs and transgenic worms. We constructed pEntry RFP by cloning mcherry RFP⁴⁵ with *SaI*I and *Eco*RI into *Xba*I-*Eco*RI sites in pEntry. We constructed pEntry YCD3 by cloning a YCD3 version of cameleon using the same cloning strategy as for RFP. (The YCD3 combines the modifications to cameleon described in refs. 46,47). A 2.4-kb *del-2* promoter fragment was obtained by PCR on *C. elegans* genomic DNA using primers 5'-GCTTCTCCCAACCGTTGTGATTC-3' and 5'-GCGAGAAGAGG AGGAGAAAAGTGATTG-3' and cloned into pDest 49.26 (ref. 48). A 4.8-kb *ocr-4* promoter fragment was similarly cloned using primers 5'-GCATGCTCA AAGACCTTGGCTCCAC-3' and 5'-GGTACCTAATACAAGTTAGATTGAGAGA-3'. We then used LR Clonase (Invitrogen) to generate *pdel-2::RFP*, *pocr-4::YCD3*, and *pocr-4::RFP*. We injected the RFP constructs at 75 ng μl^{-1} into the N2 strain, along with *unc-122::GFP* at 15 ng μl^{-1} as a marker to generate *ljEx117* and *ljEx122* respectively. We injected *pocr-4::YCD3* at 90 ng μl^{-1} into *trpa-1(ok999)* to create *ljEx130*. This was then crossed to *trp-1(ok999)*; *ljEx115[pdel-2::trpa-1; punc122::GFP]* and backcrossed to wild-type (N2). The extrachromosomal array from this transformed line was introduced into the various *trpa-1* genetic backgrounds by an isogenic genetic cross. We observed no significant effects of *trpa-1* genotype on cameleon expression, as inferred from initial fluorescence intensity or from initial ratio baseline (Supplementary Fig. 5). We also assayed the differences in touch-induced calcium influx in OLQ between *trpa-1* and wild-type worms using a second, independently generated extrachromosomal transgenic line obtained in a similar manner (data not shown). For ASH imaging, we used *lin-15(n765)*; *ljEx95[psra-6::YC2.12 lin-15(+)]* worms²⁷.

Microscopy for still images and cell identification. To collect still images we used a Zeiss AxioScope 100 microscope equipped with GFP and Texas red filters and an ORCA CCD camera. Worms were immobilized on 2% agarose pads in M9 buffer with 40 mM NaN_3 . For DiI staining, we washed worms with H_2O twice and resuspended them in 1 ml M9 with 2 μl DiI stock (2 mg ml^{-1}) for 20 min. We then washed them once with H_2O and placed them on an NGM plate with food for 20 min. Nearby unstained neurons and FLP neurons were identified by monitoring cell body position using DIC optics²⁴, by characteristic axonal morphology and by location relative to staining with the DiI.

***C. elegans* strains and genotypic analysis.** Strains were maintained under standard conditions at 20 °C, on NGM agar with OP50 *E. coli* as a food source. The wild-type reference strain used was N2 Bristol. The mutant alleles used were as follows:

LGIII: KP4 *glr-1(n2461)* LGIV: RB1052 *trpa-1(ok999)*, TM1402 *trpa-1(tm1402)*, CX10 *osm-9(ky10)* LGX: TU253 *mec-4(u253)*, MT8189 *lin-15(n765)*.

We created the following strains and arrays in this work (neuronal promoter expression is indicated; *punc-122::GFP* and *lin-15(+)* are coinjection markers):

AQ1340 *trpa-1(ok999)* IV; *mec-4(u253)* X
 TRPA-1 expression and colocalization:
 AQ1126 *lin-15(n765)* X; *ljEx107[lin-15(+); TRPA-1::GFP (2 exons)]*
 AQ1206 *lin-15(n765)* X; *ljEx109[lin-15(+); TRPA-1::GFP (6 exons)]*
 AQ1295 *ljEx114[TRPA-1::GFP (full length)]*
 AQ1346 *ljEx117[pdel-2::RFP OLQ and IL1; punc-122::GFP]*
 AQ1394 *ljEx122[pocr-4::RFP OLQ; punc-122::GFP]*
 TRPA-1 rescue:
 AQ1341 *trpa-1(ok999)* IV; *ljEx115[pdel-2::ctrpa-1(+)* OLQ and IL1; *punc-122::GFP]*
 AQ1342 *trpa-1(tm1402)* IV; *ljEx115[pdel-2::ctrpa-1(+)* OLQ and IL1; *punc-122::GFP]*
 AQ1343 *trpa-1(ok999)* IV; *ljEx121[pdel-2::mtrpa-1(+)* OLQ and IL1; *punc-122::GFP]*
 AQ1392 *trpa-1(ok999)* IV; *ljEx118[psra-6::ctrpa-1(+)* ASH; *punc-122::GFP]*
 AQ1393 *trpa-1(ok999)* IV; *ljEx119[psra-6::ctrpa-1(+)* ASH; *punc-122::GFP]*
 Calcium imaging:
 AQ1348 *trpa-1(ok999)* IV; *ljEx95[lin-15(+); psra-6::YCD2.12* ASH]
 AQ1490 *ljEx130[pocr-4::YCD3* OLQ]
 AQ1491 *trpa-1(ok999)* IV; *ljEx130[pocr-4::YCD3* OLQ]
 AQ1492 *trpa-1(ok999)* IV; *ljEx115[pdel-2::ctrpa-1(+)* OLQ and IL1; *punc-122::GFP]*; *ljEx130[pocr-4::YCD3* OLQ]

We obtained the *trpa-1* mutant strains from the *C. elegans* Genetics Center, provided by the *C. elegans* gene knockout project at Oklahoma Medical Research Facility (*ok999*), and from the Japanese National Bioresource Project (*tm1402*). The two *trpa-1* mutant alleles we obtained were outcrossed four times to the wild-type N2 strain.

Behavioral assays: For all behavioral assays, we used 4-d-old young adults unless otherwise mentioned. For additional behavioral methods see **Supplementary Methods** online.

We performed ASH avoidance assays as previously described⁴⁹. The avoidance index is the number of positive responses divided by the total number of trials⁴⁹. We performed nose-touch assays as previously described¹⁰. Assay plates were prepared fresh within 4 h of use by spreading one drop of OP50 onto plates. For each strain, ten worms were allowed to move forward into an eyelash in the path of the worm. We repeated this ten times for each worm, at least three trials per strain, and recorded either a reversal response, head withdrawal or null response. We scored the assay blinded and repeated it on at least three independent days. Nose-touch insensitive mutants *osm-9(ky10)* and *glr-1(2461)* served as a positive controls. For habituation to nose-touch, we tested worms in the same manner as described above, but gave 30 stimulations per worm.

For the inhibition of foraging in response to anterior touch, we used plates and hair picks prepared as for the nose-touch assay. Touch in this case was applied during forward movement to the top of the head or anterior body (from the first pharyngeal bulb to approximately 40 μ m from the vulva). We defined inhibition of foraging as at least two consecutive head bends without foraging during backward movement. We scored (blinded) 30 worms per strain on each trial, using the *glr-1(n2461)* mutant, defective in this behavior, as a positive control.

We carried out laser ablations on newly hatched L1 worms by standard methods. Neurons were identified using *ljEx122[pocr-4::RFP]* transgenic worms as a marker for the OLQ neurons. Worms were scored blinded as young adults. Each worm was given ten stimulations as described for the nose-touch assay. We repeated this two more times for each worm, with 1 h between sets.

To quantify the frequency of foraging, we tracked worms using a Zeiss Stemi 2000-c stereomicroscope equipped with a Cohu high performance CCD video camera recording at a capture rate of 30 frames per s. A computer-controlled tracker (Parker Automation, SMC-1N) kept the worm in view during the 1-min recording. Videos were collected on fresh, thinly seeded OP50 plates. We scored the videos blind frame-by-frame, counting the number of foraging movements in 10-s intervals during which the worm was moving forward. A foraging movement was defined as a complete cycle of movements by the tip of the nose from the ventral side through the dorsal extreme or vice versa. We quantified two 10-s intervals for each worm and scored at least 25 worms per strain.

Rescue of TRPA-1 mutant phenotype. We created *pdel-2::ctrpa-1* for labial neuron-specific rescue. Full-length *C. elegans* TRPA-1 cDNA was subcloned into the *pdel-2* pDest vector at the *KpnI-SalI* sites. We injected *trpa-1(tm1402)* mutant worms with *pdel-2::ctrpa-1* at 75 ng μ l⁻¹, along with *punc-122::GFP* as a marker at 25 ng μ l⁻¹, to create *ljEx115*. This array was crossed into *trpa-1(ok999)* to score rescue in both alleles. For the mammalian rescue construct, we subcloned full-length mouse TRPA1 cDNA into the pDest 49.26 vector containing *pdel-2* at *KpnI-SalI* sites and injected it into *trpa-1(ok999)* mutant worms at 75 ng μ l⁻¹ with *punc-122::GFP* at 15 ng μ l⁻¹ to generate *ljEx121[pdel-2::mtrpa-1]* transgenic worms. ASH-specific rescue of *trpa-1* was made by fusing a 4-kb *sra-6* promoter fragment to full-length *C. elegans* TRPA-1 cDNA cloned into pDest 49.26 at the *NheI-KpnI* site¹⁷. We injected the resulting *psra-6::trpa-1* construct in *trpa-1(ok999)* worms at 50 ng μ l⁻¹ with *punc-122::GFP* at 15 ng μ l⁻¹ to generate *ljEx118* and *ljEx119*.

In vivo calcium imaging. We used a Zeiss Axioskop 2 upright compound microscope equipped with a Dual View beam splitter (Optical Insights) and a Uniblitz Shutter (Vincent Associates). Fluorescence images were acquired using MetaVue 6.2 (Universal Imaging). We acquired images at 75 Hz for ASH and OLQ recordings, with 4 \times 4 binning, using a \times 63 Zeiss Achromplan water immersion objective. Filter-dichroic pairs were excitation, 400–440; excitation dichroic 455; CFP emission, 465–495; emission dichroic 505; YFP emission, 520–550 (Chroma). We glued individual adult worms (~24 h past L4) with Nexabond S/C cyanoacrylate glue to pads composed of 2% agarose in extracellular saline (145 mM NaCl, 5 mM KCl, 1 mM CaCl₂, 5 mM MgCl₂, 20 mM D-glucose, 10 mM HEPES buffer, pH 7.2). This saline, with the addition of 2.0 mM serotonin, was used to immerse worms before stimulation. Worms used for calcium imaging showed similar levels of cameleon expression in sensory neurons as inferred from initial fluorescence intensity (**Supplementary Fig. 5**). The nose-touch stimulator was a needle with a 50- μ m diameter made of a drawn glass capillary (1.2 mm outer diameter, 0.69 mm inner diameter borosilicate glass) with the tip rounded to ~10 μ m on a flame. We positioned the stimulator using a motorized stage (Polytec/PI M-111.1DG microtranslation stage with C-862 Mercury II controller) to stimulate nose-touch. After the worm initiated pumping, we placed the needle perpendicular to the worm's body at a distance of 150 μ m from the side of the nose. In the 'on' phase, the glass tip was moved toward the worm so that it could probe ~8 μ m into the side of the worm's nose on the cilia and held on the cilia for 2 s, and in the 'off' phase the needle was returned to its original position. We observed similar nose-touch results in ASH assays if we brought the probe in into the tip of the nose during the stimulation as was done previously²⁷. For ASH nose-touch all worms were preexposed to UV for 60 s before the initial stimulus. We analyzed images using a custom program written in Java that reported the fluorescence intensity recorded simultaneously in YFP and CFP channels. The ratiometric measure of *in vivo* calcium was then calculated as (YFP intensity)/(CFP intensity) - 0.6. This correction factor was required to correct for crosstalk of CFP emission into the YFP channel; the CFP produces a signal in the YFP channel that is 60% of that in CFP channel²⁷. Ratio changes were displayed and parameterized using scripts written in Matlab (The Mathworks) as described previously²⁷. For each strain, we recorded two responses with five minutes between stimulations, and statistically analyzed data from a number of worms ($n = 8$ worms per strain for ASH, $n = 14, 18$ and 13 for wild-type, *trpa-1* and *trpa-1+Ex115[pdel-2::ctrpa-1]* respectively for OLQ).

Electrophysiology. We generated *C. elegans* TRPA-1-expressing tet-inducible stable CHO cells as previously described¹⁵. For transient transfections CHO cells were transfected using Eugene as previously described³⁴. Cells were plated onto poly-D-lysine-coated coverslips for recording purposes, and we made recordings 24 h after tet induction. Recording electrodes were fabricated from borosilicate capillary tubing (B150-86-10; Sutter Instrument) and had resistances of 2–5 M Ω when containing intracellular saline (see below). Current signals were detected and filtered at 10 kHz with a Multiclamp 700A amplifier (Axon Instruments), digitally recorded with a DigiData 1322A laboratory interface (Axon Instruments) and PC compatible computer system, and stored for offline analysis. We used PClamp9 software (Axon Instruments) for data acquisition and analysis. For whole cell experiments, a voltage ramp protocol was used with a sampling interval of 400 μ s per channel (2.5 kHz), holding at

–60 mV for 250 ms, then ramping from –120 mV to +120 mV over 325 ms, returning to –60 mV for 250 ms after the ramp. Ramps were taken with an intersweep interval of 3 s. The regular pipette solution was (in mM) CsCl, 140; EGTA, 5; HEPES, 10; Mg-ATP, 1; titrated to pH 7.4 with CsOH. The extracellular solution contained (in mM) CsCl 140; EGTA, 5; HEPES, 10; MgCl₂, 2; and CaCl₂, 2. Pressure (positive or negative) was hydrostatically delivered by the recording pipette using a syringe and monitored through a pressure monitor (World Precision Instruments). For blocking experiments, we added 100–500 μM GdCl₃ to the extracellular solution without EGTA, as EGTA has been shown to chelate Gd³⁺ (ref. 50).

Accession codes. Wormbase: *C. elegans trpa-1*, C29E6.2; *C. elegans trpa-2*, M05B5.6. (Genbank: EF535106 and NM_059630, respectively).

Note: Supplementary information is available on the Nature Neuroscience website.

ACKNOWLEDGMENTS

We thank G. Lesa for genomic DNA and technical advice, A. Huang for his assistance with the automated worm tracker, G. Story for technical assistance and T. Jegla for assistance and discussions. We would also like to thank C. Bargmann, Rockefeller University for providing constructs and for help finding a suitable promoter to image the OLQ neurons. A. Fire (Carnegie Institution of Washington) supplied us with GFP expression vectors. We would also like to thank M. de Bono, for comments and guidance in neuronal identification. We thank the *C. elegans* gene knockout project at Oklahoma Medical Research Facility for providing the *ok999* strain, and the National Bioresource Project and the Mitani laboratory (Tokyo Women's Medical University) for providing the *tm1402* strain. This research was partially supported by US National Institutes of Health grants R01DE016927 to A.P. and R01DA016445 and R01DA018341 to W.R.S., and a Ruth Kirschstein Predoctoral Fellowship to K.S.K.

COMPETING INTERESTS STATEMENT

The authors declare no competing financial interests.

Published online at <http://www.nature.com/natureneuroscience>

Reprints and permissions information is available online at <http://npg.nature.com/reprintsandpermissions>

- Goodman, M.B. Mechanosensation. in *WormBook*, ed. The C. elegans Research Community, doi:10.1895/wormbook.1.62.1, <http://www.wormbook.org>, 6 January 2006.
- Chalfie, M. *et al.* The neural circuit for touch sensitivity in *Caenorhabditis elegans*. *J. Neurosci.* **5**, 956–964 (1985).
- Chalfie, M. & Au, M. Genetic control of differentiation of the *Caenorhabditis elegans* touch receptor neurons. *Science* **243**, 1027–1033 (1989).
- Goodman, M.B. *et al.* MEC-2 regulates *C. elegans* DEG/ENaC channels needed for mechanosensation. *Nature* **415**, 1039–1042 (2002).
- Bianchi, L. *et al.* The neurotoxic MEC-4(d) DEG/ENaC sodium channel conducts calcium: implications for necrosis initiation. *Nat. Neurosci.* **7**, 1337–1344 (2004).
- Suzuki, H. *et al.* *In vivo* imaging of *C. elegans* mechanosensory neurons demonstrates a specific role for the MEC-4 channel in the process of gentle touch sensation. *Neuron* **39**, 1005–1017 (2003).
- O'Hagan, R., Chalfie, M. & Goodman, M.B. The MEC-4 DEG/ENaC channel of *Caenorhabditis elegans* touch receptor neurons transduces mechanical signals. *Nat. Neurosci.* **8**, 43–50 (2005).
- Kaplan, J.M. & Horvitz, H.R. A dual mechanosensory and chemosensory neuron in *Caenorhabditis elegans*. *Proc. Natl. Acad. Sci. USA* **90**, 2227–2231 (1993).
- Colbert, H.A., Smith, T.L. & Bargmann, C.I. OSM-9, a novel protein with structural similarity to channels, is required for olfaction, mechanosensation, and olfactory adaptation in *Caenorhabditis elegans*. *J. Neurosci.* **17**, 8259–8269 (1997).
- Hart, A.C., Sims, S. & Kaplan, J.M. Synaptic code for sensory modalities revealed by *C. elegans* GLR-1 glutamate receptor. *Nature* **378**, 82–85 (1995).
- Alkema, M.J., Hunter-Ensor, M., Ringstad, N. & Horvitz, H.R. Tyramine functions independently of octopamine in the *Caenorhabditis elegans* nervous system. *Neuron* **46**, 247–260 (2005).
- Harbinder, S. *et al.* Genetically targeted cell disruption in *Caenorhabditis elegans*. *Proc. Natl. Acad. Sci. USA* **94**, 13128–13133 (1997).
- Pedersen, S.F., Owsianik, G. & Nilius, B. TRP channels: an overview. *Cell Calcium* **38**, 233–252 (2005).
- Patapoutian, A., Peier, A.M., Story, G.M. & Viswanath, V. ThermoTRP channels and beyond: mechanisms of temperature sensation. *Nat. Rev. Neurosci.* **4**, 529–539 (2003).
- Story, G.M. *et al.* ANKTM1, a TRP-like channel expressed in nociceptive neurons, is activated by cold temperatures. *Cell* **112**, 819–829 (2003).
- Obata, K. *et al.* TRPA1 induced in sensory neurons contributes to cold hyperalgesia after inflammation and nerve injury. *J. Clin. Invest.* **115**, 2393–2401 (2005).
- Corey, D.P. *et al.* TRPA1 is a candidate for the mechanosensitive transduction channel of vertebrate hair cells. *Nature* **432**, 723–730 (2004).
- Bautista, D.M. *et al.* TRPA1 mediates the inflammatory actions of environmental irritants and proalgesic agents. *Cell* **124**, 1269–1282 (2006).
- Kwan, K.Y. *et al.* TRPA1 contributes to cold, mechanical, and chemical nociception but is not essential for hair-cell transduction. *Neuron* **50**, 177–189 (2006).
- Viswanath, V. *et al.* Opposite thermosensor in fruitfly and mouse. *Nature* **423**, 822–823 (2003).
- Rosenzweig, M. *et al.* The *Drosophila* ortholog of vertebrate TRPA1 regulates thermotaxis. *Genes Dev.* **19**, 419–424 (2005).
- Lee, Y. *et al.* Pyrexia is a new thermal transient receptor potential channel endowing tolerance to high temperatures in *Drosophila melanogaster*. *Nat. Genet.* **37**, 305–310 (2005).
- Tracey, W.D., Wilson, R.I., Laurent, G. & Benzer, S. *painless*, a *Drosophila* Gene Essential for Nociception. *Cell* **113**, 261–273 (2003).
- White, J.G., Southgate, E., Thompson, J.N. & Brenner, S. The structure of the nervous system of *Caenorhabditis elegans*. *Phil. Trans. R. Soc. Lond. B* **314**, 1–340 (1986).
- Tobin, D. *et al.* Combinatorial expression of TRPV channel proteins defines their sensory functions and subcellular localization in *C. elegans* neurons. *Neuron* **35**, 307–318 (2002).
- Troemel, E.R., Chou, J.H., Dwyer, N.D., Colbert, H.A. & Bargmann, C.I. Divergent seven transmembrane receptors are candidate chemosensory receptors in *C. elegans*. *Cell* **83**, 207–218 (1995).
- Hilliard, M.A. *et al.* *In vivo* imaging of *C. elegans* ASH neurons: cellular response and adaptation to chemical repellents. *EMBO J.* **24**, 63–72 (2005); erratum **24**, 1489 (2005).
- Cho, H., Shin, J., Shin, C.Y., Lee, S.Y. & Oh, U. Mechanosensitive ion channels in cultured sensory neurons of neonatal rats. *J. Neurosci.* **22**, 1238–1247 (2002).
- Hamill, O.P. & McBride, D.W., Jr. Induced membrane hypo/hyper-mechanosensitivity: a limitation of patch-clamp recording. *Annu. Rev. Physiol.* **59**, 621–631 (1997).
- McBride, D.W., Jr. & Hamill, O.P. Simplified fast pressure-clamp technique for studying mechanically gated channels. *Methods Enzymol.* **294**, 482–489 (1999).
- Chakfe, Y., Zhang, Z. & Bourque, C.W. IL-1β directly excites isolated rat supraoptic neurons via upregulation of the osmosensory cation current. *Am. J. Physiol. Regul. Integr. Comp. Physiol.* **290**, R1183–R1190 (2006).
- Liedtke, W. *et al.* Vanilloid receptor-related osmotically activated channel (VR-OAC), a candidate vertebrate osmoreceptor. *Cell* **103**, 525–535 (2000).
- Macpherson, L.J. *et al.* The pungency of garlic: activation of TRPA1 and TRPV1 in response to allicin. *Curr. Biol.* **15**, 929–934 (2005).
- Bandell, M. *et al.* Noxious cold ion channel TRPA1 is activated by pungent compounds and bradykinin. *Neuron* **41**, 849–857 (2004).
- Kanzaki, M. *et al.* Molecular identification of a eukaryotic, stretch-activated nonselective cation channel. *Science* **285**, 882–886 (1999); erratum **285**, 1493 (1999).
- Nagata, K., Duggan, A., Kumar, G. & Garcia-Anoveros, J. Nociceptor and hair cell transducer properties of TRPA1, a channel for pain and hearing. *J. Neurosci.* **25**, 4052–4061 (2005).
- Sachs, F. & Yang, X.C. Block of stretch-activated ion channels in *Xenopus* oocytes by gadolinium and calcium ions. *J. Physiol. (Lond.)* **431**, 103–122 (1990).
- Xu, H., Blair, N.T. & Clapham, D.E. Camphor activates and strongly desensitizes the transient receptor potential vanilloid subtype 1 channel in a vanilloid-independent mechanism. *J. Neurosci.* **25**, 8924–8937 (2005).
- Montell, C. The TRP superfamily of cation channels. *Sci. STKE [online]* **2005**, re3 (2005).
- Walker, R.G., Willingham, A.T. & Zuker, C.S. A *Drosophila* mechanosensory transduction channel. *Science* **287**, 2229–2234 (2000).
- Roayaie, K., Crump, J.G., Sagasti, A. & Bargmann, C.I. The Gα protein ODR-3 mediates olfactory and nociceptive function and controls cilium morphogenesis in *C. elegans* olfactory neurons. *Neuron* **20**, 55–67 (1998).
- Chalfie, M. A molecular model for mechanosensation in *Caenorhabditis elegans*. *Biol. Bull.* **192**, 125 (1997).
- Zurborg, S., Yurgonias, B., Jira, J.A., Caspani, O. & Heppenstall, P.A. Direct activation of the ion channel TRPA1 by Ca²⁺. *Nat. Neurosci.* **10**, 277–279 (2007).
- Macpherson, L.J. *et al.* Noxious compounds activate TRPA1 ion channels through covalent modification of cysteines. *Nature* **445**, 541–545 (2007).
- Shaner, N.C. *et al.* Improved monomeric red, orange and yellow fluorescent proteins derived from *Discosoma* sp. red fluorescent protein. *Nat. Biotechnol.* **22**, 1567–1572 (2004).
- Palmer, A.E., Jin, C., Reed, J.C. & Tsien, R.Y. Bcl-2-mediated alterations in endoplasmic reticulum Ca²⁺ analyzed with an improved genetically encoded fluorescent sensor. *Proc. Natl. Acad. Sci. USA* **101**, 17404–17409 (2004).
- Hasan, M.T. *et al.* Functional fluorescent Ca²⁺ indicator proteins in transgenic mice under TET control. *PLoS Biol.* **2**, e163 (2004).
- Cheung, B.H., Arellano-Carbajal, F., Rybicki, I. & de Bono, M. Soluble guanylate cyclases act in neurons exposed to the body fluid to promote *C. elegans* aggregation behavior. *Curr. Biol.* **14**, 1105–1111 (2004).
- Hilliard, M.A., Bargmann, C.I. & Bazzicalupo, P. *C. elegans* responds to chemical repellents by integrating sensory inputs from the head and the tail. *Curr. Biol.* **12**, 730–734 (2002).
- Chanda, S.K. *et al.* Genome-scale functional profiling of the mammalian AP-1 signaling pathway. *Proc. Natl. Acad. Sci. USA* **100**, 12153–12158 (2003).

